Proteomic Analysis of the Increased Proteins in Peroxiredoxin Ⅱ Deficient RBCs

Hee-Young Yang and Tae-Hoon Lee†

Department of Oral Biochemistry, Dental Science Research Institute and the BK21 Project, Medical Research Center for Biomineralization Disorders, School of Dentistry, Chonnam National University, Gwangju 500-757, Korea.

ABSTRACT

Peroxiredoxin Ⅱ (Prdx Ⅱ; a typical 2-Cys Prdx) has been originally isolated from erythrocytes, and its structure and peroxidase activity have been adequately studied. Prdx Ⅱ has been reported to protect a wide range of cellular environments as antioxidant enzyme, and its dysfunctions may be implicated in a variety of disease states associated with oxidative stress, including cancer and aging-associated pathologies. But, the precise mechanism is still obscure in various aspects of aging containing ovarian aging. Identification and relative quantification of the increased proteins affected by Prdx Ⅱ deficiency may help identify novel signaling mechanisms that are important for oxidative stress-related diseases. To identify the increased proteins in Prdx $Ⅱ^{-/-}$ mice, we performed RBC comparative proteome analysis in membrane fraction and cytosolic fractions by nano-UPLC-MS^E shotgun proteomics. We found the increased 86 proteins in membrane (32 proteins) and cytosolic (54 proteins) fractions, and analyzed comparative expression pattern in healthy RBCs of Prdx $Ⅱ^{+/+}$ mice, healthy RBCs of Prdx $Ⅱ^{-/-}$ mice, and abnormal RBCs of Prdx $Ⅱ^{-/-}$ mice. These proteins belonged to cellular functions related with RBC lifespan maintain, such as cellular morphology and assembly, cell-cell interaction, metabolism, and stress-induced signaling. Moreover, protein networks among the increased proteins were analyzed to associate with various diseases. Taken together, RBC proteome may provide clues to understand the clue about redox-imbalanced diseases.

(Key words : Peroxiredoxin Ⅱ, Red blood cell, Shotgun proteomics, Canonical pathway)

INTRODUCTION

Peroxiredoxins (Prdxs, type Ⅰ~Ⅵ) are scavenger of reactive oxygen species (ROS) in various cells and exist in diverse tissues. Indeed, a range of other cellular functions have also been associated to mammalian Prdx family members, which have been shown to mediate signaling cascades leading to cell proliferation, differentiation and apoptosis (Rhee *et al*., 2001). For the conducts of these multiful roles, it reported that Prdxs are interacted with a variety of target proteins, and protect the radical-sensitive proteins (Watabe *et al*., 1995, Iwahara *et al*., 1995). But, the identification of the redox targets of Prdxs is not yet enough. Of Prdxs, peroxiredoxin Ⅱ (Prdx Ⅱ) is ubiquitously expressed in many cell types and especially is the third most abundant protein in red blood cells (RBCs). In addition, Prdx Ⅱ has been identified as diverse synonyms (thiol-specific antioxidant/protector protein, natural killer enhancing factor-B, calpromotin, torin, or band-8) based on functional and structural characteristics (Wood *et al*., 2003, Low *et al*., 2008). Several studies were reported about the roles of Prdx Ⅱ in RBCs *in vitro* and *in vivo* (Lee *et al*., 2003, Low *et al*., 2007). Prdx Ⅱ is very effective to remove hydroperoxides in the membrane surface of RBCs as a membrane-associated form (Cha *et al*., 2000), and also is capable to protect hemoglobin (Hb) accumulation and heme metabolism (Lim *et al*., 1994, Iwahara *et al*., 1995). Prdx Ⅱ deficient mice have undergone a hemolytic anemia, and increased levels of methemoglobin under hydrogen peroxide treatment (Lee *et al*., 2003).

As oxygen carriers compared with other cell types, RBCs are primary target to oxidative damage from a wide range of conditions. In normal physiological milieu, RBCs are even under constant oxidative stress. Therefore, RBCs depict a major component of the antioxidant capacity of blood through the enzymes contained in the cell, the ROS detoxification system such as thioredoxin system, glutathione system, and low-molecular weight antioxidants of RBC's membrane (Nickel *et al*., 2006, Tsantes *et al*., 2006). RBCs also permit redox buf-

* This work was supported by the National Research Foundation of Korea (NRF) grant funded by the Korea government (MEST) (No. 2011-0030763 and 2012-0000415).

† Corresponding author : Phone: +82-62-530-4842, E-mail: thlee83@chonnam.ac.kr.

fering of both the intra- and extracellular circumstances though transmembrane electron transport (Baker and Lawen, 2000). RBCs circulate in blood together with a variety of cells that can be activated in a variety of routes, and interplay with surrounding cells of other tissues or organs. Accordingly, RBCs becomes a target of xenobiotics, parasites, or crosses a tissue where an extreme production of ROS occurs (Nohl and Stolze, 1998). Under these conditions, the cell may accumulate oxidative damage that reflects the oxidative stress of other tissues and organs. For this reason, cellular markers of damaged RBCs are potential candidates for monitoring not only RBC-linked pathologies (e.g., thalassemia, sickle cell anemia) but also other pathologic conditions associated with oxidative stress and, more generally, to monitor the overall oxidative-stress status (Minetti and Malorni, 2006).

Recent studies were reported cellular components by a variety of RBC proteome in human and mouse (Kakhniashvili *et al*., 2004, Pasini *et al*., 2006, Pasini *et al*., 2008, Roux-Dalvai *et al*., 2008). However, these studies mostly focused on components of membrane and cytosolic protein identifications in normal condition. Mouse RBCs have been studied as models for infectious diseases, various symptoms of anemia, hemolysis, erythrocyte aging (Min-Oo and Gros, 2005, Kakhniashvili *et al*., 2005, De Franceschi *et al*., 2005, Bosman *et al*., 2010). Although do not directly affect RBCs, other diseases may cause RBC physiological alterations that could be advanced for diagnostic aim or to convince better understanding of a certain pathological pattern. In this context, comparative RBC proteomics between healthy and abnormal conditions involve to promote specific biomarker discovery (Pasini *et al*., 2010).

Here we describe a nano-UPLC-MS^E based label-free quantitative proteomics for the analysis of comparative RBC proteomics between Prdx $\text{II}^{+/+}$ and Prdx $\text{II}^{-/-}$ mice. To identify networks of the identified proteins, we selected membrane and cytosolic proteins increased in RBCs of Prdx $\text{II}^{-/-}$ mice compared with the control mice. In this study, we discovered that protein networks associated with increased expression were affected by Prdx II knockout, suggesting reciprocal relations in maintaining redox homeostasis of RBC.

MATERIALS AND METHODS

Animals

Prdx $\text{II}^{+/+}$ (Wt) and Prdx $\text{II}^{-/-}$ (Knockout) mice with C57BL6/J background were used in 3~24 months of age. All the mice were bred under specific-pathogen free (SPF) conditions and were cared for according to animal care regulation (ACR) of Chonnam National University. Previously, we made an intensive investigation of RBC's defects into Prdx $\text{II}^{-/-}$ mice (Lee *et al*., 2003).

RBC Fractionation

Density fractionation of RBCs was performed on discontinuous gradients of arabinogalactan (Larcoll; L0650, Sigma, St Louis, MO) as described previously (Lee *et al*., 2003). Larcoll-BSA and BSG-BSA solutions were prepared according to the manufacturer's instruction: Larcoll-BSA solution (250 g Larcoll in 400 mL distilled water and then boiling, 834 g distilled water, 23.5 g bovine serum albumin, 1.25 g glucose, 0.725 g $MgCl_2 \cdot H_2O$, and 41.3 mL 0.3 M K_2PO_4, pH 7.4) and BSG-BSA solution (4.86 g NaCl, 0.732 g Na_2HPO_4, 0.131 g NaH_2PO_4, 1.2 g glucose, 18 g BSA in 1 L distilled water); the buffers were adjusted to pH 7.4 with 1 N NaOH (290 mosm/L with NaCl). Larcoll solutions were diluted in 10 different densities ranging from 1.135 to 1.014 g/mL (62.5~100% of Larcoll) and discontinuously layered on the gradient. 10 mL blood from 20 mice was layered on top of the gradients and centrifuged for 45 min at 25,000 g at 4℃. The isolated RBCs were sorted into normal fraction (W1) of Prdx $\text{II}^{+/+}$ mice, and normal fraction (K1) and dense (K2) of Prdx $\text{II}^{-/-}$ mice (Yang *et al*., 2012). The fractionized cells were collected separately and washed three times with BSG-BSG solution (Yang *et al*., 2012). The RBC membrane was washed till colorless with hypotonic buffer (5 mM $NaPO_4$, pH 7.4, 1 mM EDTA), and collected by centrifugation at 13,000 rpm for 20 min at 4℃. And then, membrane fraction was dissolved in urea lysis buffer (7 M urea, 2 M thiourea, 0.49% (w/v) CHAPS, 10mM Tris-HCl, pH 7.4). The cytosolic proteins were gathered from the supernatant of lysate, and then purified by dialysis with PBS. Hemoglobin in cytosolic fractions was removed using Nickel-affinity column (QIAGEN). Protein concentration of membrane and cytosol fraction was determined by Bradford method (Bio-Rad Laboratories).

The RBC Proteome

In-gel Tryptic Digestion

800 μg of membrane proteins or 200 μg of cytosolic proteins were subjected to 8% SDS-PAGE, respectively. The separated proteins were then visualized by staining with Coomassie Blue (R250). For efficient trypsin treatment of proteins, the separated gels were excised by extracting 10 gel slices. And then proteins were reduced with 10 mM DTT and alkylated with 55 mM *N*-ethylmaleimide (NEM; Sigma- Aldrich) in 100 mM ammonium bicarbonate. Following tryptic digestion (2 μg/sliced gel; Promega) for 16 h at 37℃, the peptides were recovered and extracted from the sliced gels by 5% formic acid and 50% acetonitrile. The combined samples were desalted using a solid phase Oasis

HLB C18 microelution plate (Waters, Inc.) and then stored at −80℃ before being subjected to nano-LC-MS/MS analysis for comparative proteomics.

Nano-UPLC-MS^E Tandem Mass Spectrometry

The separations were performed on a 75 μm×250 mm nano-ACQUITY UPLC 1.7 μm BEH300 C18 RP column and a 180 μm×20 mm Symmetry C18 RP 5 μm enrichment column using a nano-ACQUITY Ultra Performance LC Chromatography™ System (Waters Corporation, MA, USA). For long-term ionization stability, a newly developed spray tip was used as previously reported(Chung *et al*., 2009). Tryptic digested peptides (5 μl) were loaded onto the enrichment column with mobile pahse A contained 3% acetonitrile in water with 0.1% formic acid. A step gradient was used at flow rate of 300 nL/min. This included a 3～40% mobile phase B, 97% acetonitrile in water with 0.1% formic acid, over 95 min, 40～70% mobile phase B over 20 min, followed by a sharp increase to 80% B in within 10 min. Sodium formate (1 μmol/ min) was used to calibrate the TOF analyzer in the range of m/z 50～2,000 and [Glu1]-fibrinopeptide (m/z 785.8426) at 600 nL/min was used for lock mass correction. During the data acquisition, collision energy of low energy MS mode and high energy mode (MS^E) were set to 4 eV and 15～40 eV energy ramping, respectively. One cycle of MS and MS^E mode of acquisition was performed with every 3.2 s. In each cycle, MS spectra were acquired for 1.5 s with a 0.1 s inter scan delay (m/z 300 ～1,990) and the MS^E fragmentation (m/z 50～2,000) data were collected in triplicate.

Protein Identification and Quantitative Analysis

The continuum LC-MS^E data were processed and searched using the IDENTITY^E algorithm in PLGS (ProteinLynx GlobalServer) version 2.3.3 (Waters Corporation). Acquired data from alternating low and elevated energy mode in the LC-MS^E were automatically smoothed, background subtracted, centred, deisotoped and charge state reduced and then alignment of precursor and fragmentation data were combined with retention time tolerance, ±0.05 min, using PLGS software. Processed ions were mapped against the IPI mouse database (version 3.44) using the following parameters: peptide tolerance, 100 ppm; fragment tolerance, 0.2 Da; missed cleavage, 1; and variable modifications, NEM (C; cysteine). Peptide identification was performed tryptic digestion rule with one missed cleavage. As a result, protein identification was completed with arrangement of at least two peptides. All identified proteins on the basis the IDENTITY^E algorithm are in keeping with >95% probability. The false positive rate for protein identification was set to 5% in the databank search query option based on the automatically generated reversed database in PLGS 2.3.3. Protein identification was also based on the assignment of at least two peptides with together seven fragments or more. MS^E based label-free quantitation of proteins, which was based on measurements of peptide ion peak intensities observed in low collision energy mode (MS) of a triplicate set, was carried out using Expression™ Software (version 2). For normalization of each sample, the "autonormalization" function of PLGS was used. An average fold change value of proteins was calculated with multiple tryptic peptides from each protein and each average fold change was calculated from standard deviation of the peptide ion peak intensity measurement. The total numbers of observed tryptic peptides were used to determine 95% confidence level. Finally, Expression software generated results as an EMRT (exact mass retention time) table, which contains protein peptide information and their quantitation value.

Bioinformatics Analysis

Ingenuity Pathway Analysis (IPA version 7.6～2402; Ingenuity Systems Inc., www. ingenuity.com) was used to perform a knowledge- based network and canonical-pathway analysis of the nano-LC-MS^E comparative proteomics data.

Western Blotting

The extracted protein concentration from membrane and cytosolic fraction of RBCs was determined by Bradford method. Proteins were separated on 8% polyacrylamide gel. Separated proteins were transferred onto polyvinylidene fluoride membrane, after which the membrane was incubated with the following primary antibodies: anti-UBA1 (1:1,000; Cell Signaling Technology) or anti-MTHFD1 (1:1,000; Abcam), anti-PFAS (1:1000; Abcam), or anti-KRT5 (Sigma-Aldrich) and then with HRP-conjugated secondary antibody (Cell Signaling Technology). Immunoreactive proteins were detected using an ECL system (iNtRON, South Korea).

RESULTS

Identification of Proteins Differentially Regulated in Prdx Ⅱ Deficient RBCs

Previously, we reported that Prdx Ⅱ protects RBC lifespan under oxidative stress (Lee *et al*., 2003). In Prdx Ⅱ$^{-/-}$ mice, blood contained immature reticulocytes, morphologically abnormal cells, and RBCs had highly increased ROS levels. Moreover, membrane proteins in RBCs of Prdx Ⅱ$^{-/-}$ mice were oxidatively damaged than that of Prdx Ⅱ$^{+/+}$ mice. As a consequence of

Table 1. List of differentially increased proteins in RBC's membrane fraction of Peroxiredoxin Ⅱ knockout mice

No.	IPI No.	Protein description	Gene symbol	Score (PLGS)	Ratio of expression		
					W1:K1	W1:K2	K2:K1
1	IPI00857025	AarF domain containing kinase 4	Adck4	151.22	-	K2	K2
2	IPI00123183	Aquaporin-1	Aqp1	190.54	-	K2	K2
3	IPI00467336	Isoform 1 of Rho GTPase-activating protein 6	Arhgap6	368.39	K1	-	K1
4	IPI00224036	Butyrophilin-like protein Butr-1 homolog	Butrl1	197.24	-	K2	K2
5	IPI00129197	M-phase inducer phosphatase 2	Cdc25b	170.82	-	K2	K2
6	IPI00461304	ATP-dependent RNA helicase	Dhx8	1,117.05	-	K2	K2
7	IPI00225940	Dynein, axonemal, light intermediate polypeptide 1	Dnali1	110.51	K1	-	K1
8	IPI00473227	Alpha non-neuron	Eno1	132.27	K1	K2	3.67
9	IPI00122684	Gamma-enolase	Eno2	113.64	K1	K2	3.35
10	IPI00125328	Dematin	Epb4.9	420.96	-	K2	K2
11	IPI00228385	Glucose-6-phosphate 1-dehydrogenase X	G6pdx	238.46	K1	K2	2.12
12	IPI00117042	Isoform 1 of Glial fibrillary acidic protein	Gfap	217.61	-	K2	K2
13	IPI00124954	Kinesin-1 heavy chain	Kif5b	504.87	K1	-	K1
14	IPI00323881	Importin subunit beta-1	Kpnb1	290.88	-	K2	K2
15	IPI00876179	Keratin, type I cytoskeletal 15	Krt15	254.92	K1	-	K1
16	IPI00556722	Mitogen-activated protein kinase 11	Mapk11	125.17	-	K2	K2
17	IPI00122862	C-1-tetrahydrofolate synthase, cytoplasmic	Mthfd1	367.57	K1	K2	1.65
18	IPI00756332	Zinc finger protein 120-like	-	149.95	-	K2	K2
19	IPI00119305	Proliferation-associated protein 2G4	Pa2g4	259.42	-	K2	K2
20	IPI00323483	Isoform 3 of Programmed cell death 6-interacting protein	Pdcd6ip	326.97	K1	-	K1
21	IPI00230108	Protein disulfide-isomerase A3	Pdia3	284.1	K1	-	K1
22	IPI00775829	Pyruvate kinase isozymes R/L isoform 2	Pklr	270.32	K1	-	K1
23	IPI00123494	26S proteasome non-ATPase regulatory subunit 2	Psmd2	502.81	0.48	0.39	1.23
24	IPI00120761	Isoform Erythrocyte of Band 3 anion transport protein	Slc4a1	2,739.81	0.44	0.30	0.70
25	IPI00459493	Isoform 1 of T-complex protein 1 subunit alpha	Tcp1	216.32	K1	-	K1
26	IPI00123313	Ubiquitin-like modifier-activating enzyme 1	Uba1	560.06	-	K2	K2
27	IPI00138892	Ubiquitin-60S ribosomal protein L40	Uba52	329.03	0.21	0.13	1.62
28	IPI00139518	Polyubiquitin-B	Ubb	409.93	0.12	0.08	1.62
29	IPI00750889	Polyubiquitin-C	Ubc	516.41	K1	K2	1.63
30	IPI00453803	Ubiquitin-conjugating enzyme E2 O	Ube2o	465.98	K1	-	K1
31	IPI00881918	Ubiquitin carboxyl-terminal hydrolase	Usp5	347.23	K1	-	K1
32	IPI00116444	Zinc finger protein 639	Zfp639	149.41	K1	-	K1

-, not detected in proteomic quantiation.

physiological changes, dense cells were increased and contained about 30% of Heinz bodies in Prdx $\text{Ⅱ}^{-/-}$ than that of Prdx $\text{Ⅱ}^{+/+}$ mice (Yang *et al*., 2012). These data indicate that RBC proteins were also damaged by Prdx Ⅱ deficiency.

Because Prdx Ⅱ as antioxidant enzyme protects specific RBC proteins under oxidative stress condition, we next identified proteins differently regulated between

Table 2. List of differentially increased proteins in RBC's cytosolic fraction of Peroxiredoxin Ⅱ knockout mice

No.	IPI No.	Protein description	Gene symbol	Score (PLGS)	Ratio of expression		
					W1:K1	W1:K2	K2:K1
1	IPI00126940	Isoform long of Adenosine kinase	Adk	197.38	K1	-	K1
2	IPI00153740	Activator of 90 kDa heat shock protein ATPase homolog 1	Ahsa1	313.43	K1	-	K1
3	IPI00649528	Asparagine-linked glycosylation 6 homolog	Alg6	99.27	-	K2	K2
4	IPI00322312	Rho GDP-dissociation inhibitor 1	Arhgdia	231.69	0.58	W1	K1
5	IPI00407692	Isoform 1 of V-type proton ATPase catalytic subunit A	Atp6v1a	333.80	-	K2	K2
6	IPI00649994	Adenylate cyclase-associated protein 1	Cap1	88.41	0.59	W1	K1
7	IPI00626909	Calpain-1 catalytic subunit	Capn1	529.16	K1	-	K1
8	IPI00121534	Carbonic anhydrase 2	Car2	886.78	0.89	0.39	2.27
9	IPI00120113	UMP-CMP kinase 2, mitochondrial	Cmpk2	273.57	K1	-	K1
10	IPI00226569	Isoform 1 of Uncharacterized protein C7orf46 homolog	D330028D13Rik	112.57	-	K2	K2
11	IPI00122743	Aspartyl-tRNA synthetase, cytoplasmic	Dars	408.46	0.52	W1	K1
12	IPI00267960	Deoxycytidylate deaminase	Dctd	114.04	-	K2	K2
13	IPI00153463	Dehydrogenase/reductase SDR family member 11	Dhrs11	241.29	K1	-	K1
14	IPI00228601	Isoform 2 of DNA methyltransferase 1-associated protein 1	Dmap1	213.78	K1	-	K1
15	IPI00466069	Elongation factor 2	Eef2	415.58	K1	-	K1
16	IPI00342382	Exosome component 10	Exosc10	369.97	-	K2	K2
17	IPI00330862	Ezrin	Ezr	481.82	K1	K2	1.65
18	IPI00119019	Coagulation factor XI	F11	219.72	-	K2	K2
19	IPI00228867	Glucose-6-phosphate 1-dehydrogenase 2	G6pd2	229.08	-	K2	K2
20	IPI00117042	Isoform 1 of Glial fibrillary acidic protein	Gfap	245.93	-	K2	K2
21	IPI00132126	Hairy/enhancer-of-split related with YRPW motif protein 2	Hey2	118.9	W1	0.29	K2
22	IPI00133916	Heterogeneous nuclear ribonucleoprotein H	Hnrph1	199.32	K1	-	K1
23	IPI00229883	Isoform 1 of Integrator complex subunit 4	Ints4	365.09	K1	-	K1
24	IPI00755029	Intersectin 1 isoform 3	Itsn1	286.14	K1	-	K1
25	IPI00652843	Lysine-specific demethylase 5B	Kdm5b	289.20	-	K2	K2
26	IPI00742334	Importin (karyopherin) subunit beta-1	Kpnb1	484.56	0.53	W1	K1
27	IPI00881933	SKI family transcriptional corepressor 1	Skor1	372.28	-	K2	K2
28	IPI00229527	Leukotriene A-4 hydrolase	Lta4h	278.62	K1	-	K1
29	IPI00126148	Transcription factor MafK	Mafk	92.11	K1	-	K1
30	IPI00122862	C-1-tetrahydrofolate synthase, cytoplasmic	Mthfd1	686.37	0.55	W1	K1
31	IPI00551485	Nucleoside diphosphate kinase A	Nme1	208.51	K1	-	K1
32	IPI00127417	Nucleoside diphosphate kinase B	Nme2	131.71	K1	-	K1
33	IPI00131299	Isoform 1 of Cone cGMP-specific 3',5'-cyclic phosphodiesterase subunit alpha'	Pde6c	409.02	K1	-	K1
34	IPI00555060	Phosphoglycerate kinase 2	Pgk2	267.78	K1	-	K1
35	IPI00129096	Pyridoxine-5'-phosphate oxidase	Pnpo	167.73	K1	-	K1
36	IPI00129319	Protein phosphatase 1 regulatory subunit 7	Ppp1r7	196.63	K1	-	K1
37	IPI00121788	Peroxiredoxin 1	Prdx1	164.02	K1	-	K1
38	IPI00622983	Isoform 1 of Prominin-2	Prom2	289.31	-	K2	K2
39	IPI00881789	Pleckstrin and Sec7 domain containing 3 isoform 3	Psd3	207.47	K1	-	K1
40	IPI00828513	26S protease regulatory subunit 6B	Psmc4	294.67	K1	-	K1
41	IPI00222515	26S proteasome non-ATPase regulatory subunit 11	Psmd11	182.87	K1	-	K1
42	IPI00225337	Retinol-binding protein 1	Rbp1	86.97	-	K2	K2
43	IPI00112377	Retinol dehydrogenase 14	Rdh14	101.77	K1	-	K1
44	IPI00124066	Isoform 2 of Paired amphipathic helix protein	Sin3b	82.85	-	K2	K2
45	IPI00857616	Isoform 3 of Sperm flagellar protein 2	Spef2	200.74	K1	-	K1
46	IPI00124116	Isoform 1 of Histone-lysine N-methyltransferase	Suv39h1	136.67	-	K2	K2
47	IPI00720182	Isoform 2 of Tolloid-like protein 1	Tll1	199.28	K1	-	K1
48	IPI00881225	Tumor protein D52	Tpd52	115.97	K1	-	K1
49	IPI00132762	Heat shock protein 75 kDa, mitochondrial	Trap1	356.61	K1	-	K1
50	IPI00881922	Isoform 2 of Tetratricopeptide repeat protein 23	Ttc23	206.76	K1	-	K1
51	IPI00754663	Ubiquitin-conjugating enzyme E2L 6	Ube2l6	207.34	K1	-	K1
52	IPI00830493	UDP glycosyltransferase 1 family, polypeptide A10	Ugt1a10	108.32	K1	-	K1
53	IPI00113738	Isoform 1 of Tryptophanyl-tRNA synthetase, cytoplasmic	Wars	224.35	K1	-	K1
54	IPI00844705	X-linked lymphocyte-regulated 4B	Xlr4b	115.13	K1	-	K1

-, not detected in proteomic quantiation.

Table 3. The associated network functions generated by the Ingenuity Pathway Analysis

Name[a]	Score	No. of molecules	Molecules
14-3-3, 19S proteasome, 26s Proteasome, Actin, Akt, **CA2**, **CAP1**, **CAPN1**, **CDC-25B**, Ck2, Cyclin A, **DARS**, **EEF2**, **G6PD**, **GFAP**, Insulin, **ITSN1**, **KIF5B**, **NME1**, **NME2**, **PA2G4**, **PDCD6IP**, **PPP1R7**, **PSMC4**, **PSMD2**, **PSMD11**, **RBP1**, **SLC4A1**, **TPD52**, **UBA1**, **Ubb**, **UBC**, Ubiquitin, **USP5**, **WARS**	63	26	Cell Death, Cell Morphology, Infectious Disease
AHSA1, **AQP1**, **ATP6V1A**, ATP6V1D, BLVRB, CRB3, **DHX8**, EPO, ERBB2, **EXO-SC10**, FOXRED1, **G6pd2**, HNF4A, **INTS4**, KLHDC3, **KPNB1**, MCCC1, NPNT, **PDE-6C**, PEX16, **PNPO**, RSPH3, **SKOR1**, SLC31A1, SMAD3, SP1, SQRDL, TCIRG1, Timd2, TMEM43, **UGT1A8** (includes others), UGT2A3, WDR48, **ZNF639**, ZNHIT6	25	13	Gene Expression, Cell-To-Cell Signaling and Interaction, Cellular Assembly and Organization
AHSP, Androgen-AR, Ap1, **ARHGDIA**, **CMPK2**, DBC1, **DMAP1**, ELP3, ELP4, ELP5, ELP6, **ENO1**, ERMAP, **EZR**, F Actin, Histone h3, Histone h4, HMBS, Ifi47, IFNA2, **MAFK**, **MAPK11**, miR-9, NFE2L3, PARP10, Pkc(s), **PKLR**, **PRDX1**, RNA polymerase Ⅱ, RPL12, SETD2, **SUV39H1**, TBC1D10A, **UBE2L6**, ZNF622	21	11	Decreased Levels of Albumin, Gene Expression, Cellular Compromise
ADCK4, API5, ATP, BRWD1, CIDEC, **DCTD**, **DNALI1**, **ENO2**, ENO3, FGF2, FXYD-2, Gm4617/Ptma, HTT, KCTD17, KRT15, LNX1, **MTHFD1**, MYL1, MYL4, MYT1L, NDUFS7, NR3C1, **PGK2**, Pgk, SEPP1, **SIN3B**, SMARCA4, ST3GAL2, **TCP1**, TNNI-2, **TRAP1**, TXNDC11, **UBE2O**, WAC, ZMYND8	20	11	Cellular Assembly and Organization, Cellular Compromise, DNA Replication, Recombination and Repair
ADK, **ARHGAP6**, ART1, CA4, CNN2, Collagen type I, D-glucose, **EPB49**, ERK, F-2, F11, **Gm11808/Uba52**, GPR55, G α q/o, **HEY2**, HTR2, **KDM5B**, KLHDC10, LOXL-2, **LTA4H**, MIA3, miR-377 (human, mouse), NMUR1, P2RX6, **PDIA3**, PLC, Plcd2, PLCD3, PLCH2, PLCZ1, **PSD3**, SLC39A6, TGFB1, **TLL1**, XPNPEP2	19	11	Cell Death, Hematological System Development and Function, Carbohydrate Metabolism
miR-483-3p/miR-483, **PROM2**	2	1	Cancer, Hepatic System Disease, Genetic Disorder
alcohol dehydrogenase, **RDH14**, RDH	2	1	Drug Metabolism, Lipid Metabolism, Small Molecule Biochemistry

[a] Bold indicates the identified proteins in Table 1 and 2.

Prdx Ⅱ$^{+/+}$ and Prdx Ⅱ$^{-/-}$ mice. The extracted proteins were extracted from the fractionated RBCs, and subjected to in-gel trypsin digestion, after which the digested peptides were separated and analyzed using a nano-UPLC coupled Q-TOF tandem mass spectrometer. This proteomics was verified by acquired accurate data analysis based on stably continuous switching of MS^E technology and adequate possibility of relative quantitation obtained in separate chromatography runs for each sample (Roux-Dalvai *et al*., 2008). The rationale of relative quantitation without previous incorporation of stable isotope tags of amino acids is based on measuring peak chromatography runs for each sample (Xu *et al*., 2008). The validity of the relative quantitation was improved by analyzing the samples in triplicate runs, which can also provide the information about the data quality, such as replication rates among repeated runs and the confidence and reproducibility of protein identification. On the basis of these data, we identified 166, 130, and 124 of membrane proteins, and 352, 311, and 155 of cytosolic proteins in W1, K1, and K2 (with confidence level > 95%, data not shown), respectively. To identify specific targets for compensation by Prdx Ⅱ deficiency, we selected the increased proteins in Prdx Ⅱ$^{-/-}$ RBCs. We found 32 membrane (Table 1) and 54 cytosolic (Table 2) proteins increased in Prdx Ⅱ$^{-/-}$ RBCs than Prdx Ⅱ$^{+/+}$ RBCs. These proteins were classified as cellular maintenance-related proteins containing cellular morphology and assembly, cell-cell interaction, metabolism, and stress-induced signaling.

Protein Network Comprised of Identified Proteins Regulated By Prdx Ⅱ Deficiency

Proteomics data were applied to IPA to visualize complete signaling pathways for correlation between identi-

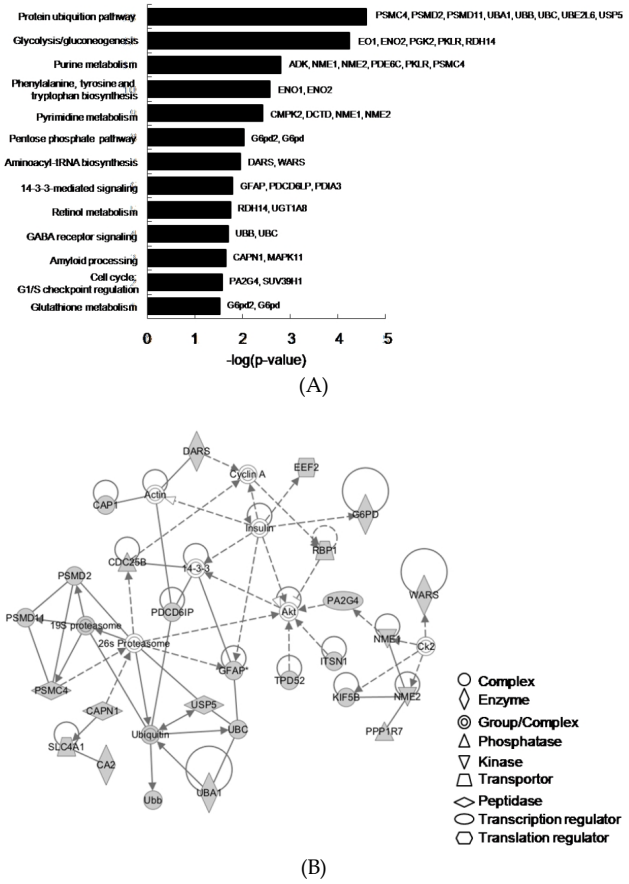

Fig. 1. Functional annotation of 86 proteins increased in Prdx Ⅱ$^{-/-}$ RBCs using IPA. (A) Top canonical networks among 32 membrane and 54 cytosolic proteins increased in Prdx Ⅱ$^{-/-}$ RBCs. To categorize identified proteins, *p*-values were used to show the ratio between the number of identified proteins classified and the total number of proteins referenced in the linked function by the software. (B) The representative annotation of reciprocal network. The most significant connection in the global network of identified cysteine oxidation-sensitive proteins (Table 3) is indicated. The identified proteins in this study are shown as gray-filled figures. Solid lines indicate direct protein-protein interactions; solid arrow lines, membership or protein-DNA interactions; and dotted arrow lines, direct expressional activation.

fied proteins. Most of the identified proteins strongly correlated with pathways involving Prdx Ⅱ. With respect to damaged effects by Prdx Ⅱ deficiency, expression of the majority of proteins were categorized as cellular compensation directly triggered by oxidative stress-related cellular dysfunction, suggesting their up-regulated expression was to remove the damaged proteins. The cellular canonical pathways outlined Fig. 1A show that most of these proteins belonged to protein ubiquitination and metabolic (glycolysis, and amino acid and nucleic acid-associated) related enzymes. The components of main network in associated network functions were multi-connected with cell death, morphology, and cellular assembly and organization (Table 3).

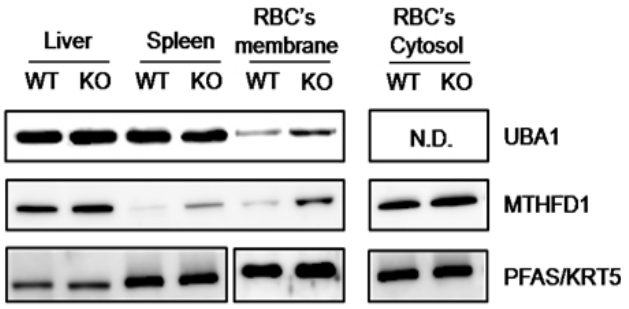

Fig. 2. Western blot analysis verifying the expression levels of proteins increased by Prdx Ⅱ deficient RBCs. The expression of UBA1 and MTHFD1 were confirmed in liver, spleen, and RBCs of Prdx Ⅱ WT and KO. Samples were run in triplicate; PFAS served as a loading control in liver, spleen, RBC's cytosolic fraction; KRT5 served as a loading control in RBC's membrane fraction. WT, Prdx Ⅱ$^{+/+}$ mice; KO, Prdx Ⅱ$^{-/-}$ mice. N.D., not detected in western blotting.

Fig. 1B is a multi-directed interaction network between the increased target proteins in membrane and cytosolic fraction determined to have the most significantly related functions. Interestingly, we found that expression of a number of proteins related to infectious disease was significantly affected in Prdx Ⅱ$^{-/-}$ RBCs, potentially disrupting the immune response under chronic oxidative stress. And based on the unique function of RBC, we suggest Prdx Ⅱ deficiency also likely affected morphological abnormality.

Verification of the Expressional Changes in Prdx Ⅱ$^{-/-}$ RBCs

To verify the results of the proteomics analysis, we compared the results of the proteomics-based resolution with western blotting. Following the proteomics and bioinformatics studies (Fig. 1A), the expression pattern of proteins involved in ubiquitination and metabolism were compared in liver, spleen, and RBC of Prdx Ⅱ$^{+/+}$ and Prdx Ⅱ$^{-/-}$ mice. UBA1 (IPI00123313, ubiquitin-like modifier-activating enzyme 1) were higher in membrane fraction of Prdx Ⅱ$^{-/-}$ RBCs than Prdx Ⅱ$^{+/+}$ RBCs (Fig. 2), which is consistent with MS data (Table 1). But, UBA1 was not changed in liver and spleen of Wt and KO mice. With expressional alteration in both membrane and cytosolic fraction, MTHFD1 (IPI00122862, C-1-tetrahydrofolate synthase, cytoplasmic) were increased in spleen and RBCs of Prdx Ⅱ$^{-/-}$ mice, and not changed in liver (Fig. 2).

DISCUSSION

Previously, the disruption of Prdx Ⅱ protein consequently causes a hemolytic disorder. And abnormally

morphological RBC cells exist in peripheral blood stream, which are spherocytes, burr cells, schistocytes, and polychromatophilic macrocytes (Lee *et al*., 2003). These damaged cells were fractionized because of dense cells containing heinz body, aggregated hemoglobins and oxidized proteins by discontinuous gradients of arabinogalactan. As these abnormal cells were observed in a variety of diseases (Steinberg, 2008), it is important to scrutinize the alteration of intracellular molecules. For examples, abnormal RBC phenotype in hemolysis is connected with various defects in the RBC membrane expression of cytoskeletal proteins, such as ankyrin, band 3, and protein 4.1/4.2 (Peters *et al*., 1996, Shi *et al*., 1999). And also, the expression of RBC membrane proteins, related to cytoskeleton, chaperone, antioxidant, and catabolism, have been altered in sickle cell disease (Pasini *et al*., 2010). With no production of new proteins, RBC is important to protect certain intracellular proteins during blood stream circulation. Therefore, RBC has protective system to induce proteolysis in order to remove the damaged protein complexes. Experimental evidence indicates that erythrocyte can neutralize moderate amounts of free alpha globin through generalized protein quality control mechanisms, including molecular chaperones, the ubiquitin-proteasome system, and autophagy. In many ways, β-thalassemia resembles protein aggregation disorders of the nervous system, liver, and other tissues, which occur when levels of unstable proteins overtake cellular compensatory mechanisms (Khandros and Weiss, 2010). In our study, we focused the increased proteins in RBCs of Prdx Ⅱ$^{-/-}$ mice than Prdx Ⅱ$^{+/+}$ mice. These proteins were analyzed to associate with inflammatory disease, hematological disease, immunological disease, and genetic disorder. Thus, these results suggest that the highly interconnected network likely represents significantly interconnected biological functions involved in the pathogenesis of diverse diseases.

The ovaries of mammals, including those of humans and farm animals, release a constant small number of oocytes in every cycle. The majority of follicles (99.9%) selectively undergo atresia during follicular growth and development. In most mammals, follicular atresia is primarily induced by apoptosis of granulosa cells (Tilly *et al*., 1991). ROS are produced and involved in follicular atresia (Broekmans *et al*., 2007). Resent study reported that Prdx Ⅱ plays a key antioxidant role in the maturation of oocytes and development of early embryos, thus providing crucial experimental evidence for further exploring the function of Prdx Ⅱ in the development of oocytes and preimplantation embryos (Wang *et al*., 2010). And also, Prdx Ⅱ plays a pivotal role in protecting granulosa cells from ROS damage through NFKB and IKB actions (Yang *et al*., 2011). The action of Prdx Ⅱ in molecular mechanism and networks are still unclear. Therefore, our study about homeostasis by Prdx Ⅱ will help to study the ovary aging in balancing the internal microenvironment of the follicle and its ability to inhibit the follicle atresia.

The ubiquitin-activating enzyme UBA1 (E1) regulates the first step of ubiquitination, was used ATP to adenylate and then bind an ubiquitin molecule (Hershko and Ciechanover, 1998). Genetic and chemical inhibition of UBA1 induced cell death in malignant cells preferentially over normal cells, and delayed tumor growth in a mouse model of leukemia by eliciting endoplasmic reticulum (ER) stress (Xu *et al*., 2010). Thus, inhibition of UBA1 may be novel target for the treatment of hematologic malignancies. C1-tetrahydrofolate (THF) synthase (MTHFD1, methylenetetrahydrofolate dehydrogenase 1) is a trifunctional enzyme that contains cytoplasmic methylene- THF dehydrogenase, methenyl-THF cyclohydrolase and formyl C1-tetrahydrofolate synthetase activities (FTHFS). This enzyme is utilized in the de novo synthesis of thymidylate and the methionine cycle, which is essential for DNA synthesis (MacFarlane *et al*., 2011). If folate availability is continuously limited, an uncontrolled repair cycle can cause frequent breaks in DNA molecule and chromosome damage, resulting in malignant cell change, contributing to cancer development (Mostowska *et al*., 2011). Although, UBA1 and MTHFD1 were increased in RBCs of Prdx Ⅱ$^{-/-}$ mice than Prdx Ⅱ$^{+/+}$ mice, their function in RBCs under chronic oxidative stress was not identified yet. Their identities in damaged RBCs need to be further confirmed. Taken together, our network analysis will provide the clue about the pathogenesis of a variety of redox-related disease.

REFERENCES

1. Baker MA, Lawen A (2000): Plasma membrane NADH-oxidoreductase system: a critical review of the structural and functional data. Antioxidants & Redox Signaling 2:197-212.
2. Bosman GJ, Lasonder E, Groenen-Dopp YA, Willekens FL, Werre JM, Novotny VM (2010): Comparative proteomics of erythrocyte aging *in vivo* and *in vitro*. Journal of Proteomics 73:396-402.
3. Broekmans FJ, Knauff EA, Te Velde ER, Macklon N S, Fauser BC (2007): Female reproductive ageing: current knowledge and future trends. Trends in Endocrinology and Metabolism: TEM 18:58-65.
4. Cha MK, Yun CH, Kim IH (2000): Interaction of human thiol-specific antioxidant protein 1 with erythrocyte plasma membrane. Biochemistry 39:6944-6950.
5. Chung Y, Park C, Kwon J, Kim S (2009): A fused silica micro-electrospray tip with an electrically floating metal wire insert to achieve more stable

electrospray ionization. J Am Soc Mass Spectrom 20:751-754.
6. De Franceschi L, Rivera A, Fleming MD, Honczarenko M, Peters LL, Gascard P, Mohandas N, Brugnara C (2005): Evidence for a protective role of the Gardos channel against hemolysis in murine spherocytosis. Blood 106:1454-1459.
7. Hershko A, Ciechanover A (1998): The ubiquitin system. Annual Review of Biochemistry 67:425-479.
8. Iwahara S, Satoh H, Song DX, Webb J, Burlingame AL, Nagae Y, Muller-Eberhard U (1995): Purification, characterization, and cloning of a heme-binding protein (23 kDa) in rat liver cytosol. Biochemistry 34:13398-13406.
9. Kakhniashvili DG, Bulla LA, Jr. & Goodman SR (2004): The human erythrocyte proteome: analysis by ion trap mass spectrometry. Molecular & Cellular Proteomics : MCP 3:501-509.
10. Kakhniashvili DG, Griko NB, Bulla LA, Jr. & Goodman SR (2005): The proteomics of sickle cell disease: profiling of erythrocyte membrane proteins by 2D-DIGE and tandem mass spectrometry. Experimental Biology and Medicine 230:787-792.
11. Khandros E, Weiss MJ (2010): Protein quality control during erythropoiesis and hemoglobin synthesis. Hematology/oncology Clinics of North America 24:1071-1088.
12. Lee TH, Kim SU, Yu SL, Kim SH, Park DS, Moon HB, Dho SH, Kwon KS, Kwon HJ, Han YH, Jeong S, Kang SW, Shin HS, Lee KK, Rhee SG, Yu DY (2003): Peroxiredoxin Ⅱ is essential for sustaining life span of erythrocytes in mice. Blood 101:5033-5038.
13. Lim YS, Cha MK, Yun CH, Kim HK, Kim K, Kim I H (1994): Purification and characterization of thiol-specific antioxidant protein from human red blood cell: a new type of antioxidant protein. Biochem Biophys Res Commun 199:199-206.
14. Low FM, Hampton MB, Peskin AV, Winterbourn CC (2007): Peroxiredoxin 2 functions as a noncatalytic scavenger of low-level hydrogen peroxide in the erythrocyte. Blood 109:2611-2617.
15. Low FM, Hampton MB, Winterbourn CC (2008): Peroxiredoxin 2 and peroxide metabolism in the erythrocyte. Antioxid Redox Signal 10:1621-1630.
16. Macfarlane AJ, Perry CA, Mcentee MF, Lin DM, Stover PJ (2011): Mthfd1 is a modifier of chemically induced intestinal carcinogenesis. Carcinogenesis 32: 427-433.
17. Min-Oo G, Gros P (2005): Erythrocyte variants and the nature of their malaria protective effect. Cellular Microbiology 7:753-763.
18. Minetti M, Malorni W (2006): Redox control of red blood cell biology: the red blood cell as a target and source of prooxidant species. Antioxidants & Redox Signaling 8:1165-1169.
19. Mostowska A, Myka M, Lianeri M, Roszak A, Jagodzinski PP (2011): Folate and choline metabolism gene variants and development of uterine cervical carcinoma. Clinical Biochemistry 44:596-600.
20. Nickel C, Rahlfs S, Deponte M, Koncarevic S, Becker K (2006): Thioredoxin networks in the malarial parasite Plasmodium falciparum. Antioxidants & Redox Signaling 8:1227-1239.
21. Nohl H, Stolze K (1998): The effects of xenobiotics on erythrocytes. General Pharmacology 31:343-347.
22. Pasini EM, Kirkegaard M, Mortensen P, Lutz HU, Thomas AW, Mann M (2006): In-depth analysis of the membrane and cytosolic proteome of red blood cells. Blood 108:791-801.
23. Pasini EM, Kirkegaard M, Salerno D, Mortensen P, Mann M, Thomas AW (2008): Deep coverage mouse red blood cell proteome: a first comparison with the human red blood cell. Molecular & Cellular Proteomics : MCP 7:1317-1330.
24. Pasini EM, Lutz HU, Mann M, Thomas AW (2010): Red blood cell (RBC) membrane proteomics--Part Ⅱ: Comparative proteomics and RBC patho-physiology. Journal of Proteomics 73:421-435.
25. Peters LL, Shivdasani RA, Liu SC, Hanspal M, John KM, Gonzalez JM, Brugnara C, Gwynn B, Mohandas N, Alper SL, Orkin SH, Lux SE (1996): Anion exchanger 1 (band 3) is required to prevent erythrocyte membrane surface loss but not to form the membrane skeleton. Cell 86:917-927.
26. Rhee SG, Kang SW, Chang TS, Jeong W, Kim K (2001): Peroxiredoxin, a novel family of peroxidases. IUBMB Life 52:35-41.
27. Roux-Dalvai F, Gonzalez De Peredo A, Simo C, Guerrier L, Bouyssie D, Zanella A, Citterio A, Burlet-Schiltz O, Boschetti E, Righetti PG, Monsarrat B (2008): Extensive analysis of the cytoplasmic proteome of human erythrocytes using the peptide ligand library technology and advanced mass spectrometry. Molecular & Cellular Proteomics : MCP 7:2254-2269.
28. Shi ZT, Afzal V, Coller B, Patel D, Chasis JA, Parra M, Lee G, Paszty C, Stevens M, Walensky L, Peters LL, Mohandas N, Rubin E, Conboy JG (1999): Protein 4.1R-deficient mice are viable but have erythroid membrane skeleton abnormalities. The Journal of Clinical Investigation 103:331-340.
29. Steinberg MH (2008) Sickle cell anemia, the first molecular disease: overview of molecular etiology, pathophysiology, and therapeutic approaches. The Scientific World Journal 8:1295-1324.
30. Tilly JL, Kowalski KI, Johnson AL, Hsueh AJ (1991): Involvement of apoptosis in ovarian follicular atresia and postovulatory regression. Endocrinology 129: 2799-2801.
31. Tsantes AE, Bonovas S, Travlou A, Sitaras NM (2006): Redox imbalance, macrocytosis, and RBC homeostasis. Antioxidants & Redox Signaling 8:1205-1216.

32. Wang S, Huang W, Shi H, Lin C, Xie M, Wang J (2010): Localization and expression of peroxiredoxin Ⅱ in the mouse ovary, oviduct, uterus, and preimplantation embryo. Anatomical Record 293:291-297.
33. Watabe S, Hasegawa H, Takimoto K, Yamamoto Y, Takahashi SY (1995): Possible function of SP-22, a substrate of mitochondrial ATP-dependent protease, as a radical scavenger. Biochem Biophys Res Commun 213:1010-1016.
34. Wood ZA, Schroder E, Robin Harris J, Poole LB (2003): Structure, mechanism and regulation of peroxiredoxins. Trends Biochem Sci 28:32-40.
35. Xu D, Suenaga N, Edelmann MJ, Fridman R, Muschel RJ, Kessler BM (2008): Novel MMP-9 substrates in cancer cells revealed by a label-free quantitative proteomics approach. Molecular & Cellular Proteomics : MCP 7:2215-2228.
36. Xu GW, Ali M, Wood TE, Wong D, Maclean N, Wang X, Gronda M, Skrtic M, Li X, Hurren R, Mao X, Venkatesan M, Beheshti Zavareh R, Ketela T, Reed JC, Rose D, Moffat J, Batey RA, Dhe-Paganon S, Schimmer AD (2010): The ubiquitin-activating enzyme E1 as a therapeutic target for the treatment of leukemia and multiple myeloma. Blood 115: 2251-2259.
37. Yang HY, Kwon J, Choi HI, Park SH, Yang U, Park HR, Ren L, Chung KJ, Kim YU, Park BJ, Jeong SH, Lee TH (2012) In-depth analysis of cysteine oxidation by the RBC proteome: advantage of peroxiredoxin Ⅱ knockout mice. Proteomics 12:101-112.
38. Yang S, Luo A, Hao X, Lai Z, Ding T, Ma X, Mayinuer M, Shen W, Wang X, Lu Y, Ma D, Wang S (2011): Peroxiredoxin 2 inhibits granulosa cell apoptosis during follicle atresia through the NFKB pathway in mice. Biology of Reproduction 84:1182-1189.
(Received: 19 March 2012 / Accepted: 26 March 2012)